A half-wave electromagnetic energy-harvesting tie towards safe and intelligent rail transportation

Article *in* Applied Energy · May 2022

DOI: 10.1016/j.apenergy.2022.118844

3 authors, including:

Yu Pan
Virginia Polytechnic Institute and State University
18 PUBLICATIONS **174** CITATIONS

Applied Energy 313 (2022) 118844

Contents lists available at ScienceDirect

Applied Energy

journal homepage: www.elsevier.com/locate/apenergy

A half-wave electromagnetic energy-harvesting tie towards safe and intelligent rail transportation

Yu Pan [1,*], Lei Zuo [2], Mehdi Ahmadian [3]

Department of Mechanical Engineering, Virginia Tech, Blacksburg, VA 24061, USA

HIGHLIGHTS

- An innovative energy harvesting tie is designed to improve railroad safety.
- A novel ball screw based mechanical motion half-wave rectifier is proposed.
- A nonlinear model is developed to understand dynamics and predict performance.
- Test results show 16.1–44.5 W average power with field-recorded displacements.

ARTICLE INFO

Keywords:
Railroad energy harvesting
Railroad tie
Mechanical motion half-wave rectification
Ball screw

ABSTRACT

This paper presents the design, modeling, and experimental testing of a novel railroad energy harvesting tie for improving rail safety and connectivity and bringing intelligence to the railroad. The system is intended for applications that require trackside power in remote locations and tunnels, where electrical power for wayside safety equipment, wireless communication systems, and health monitoring systems is needed but difficult to supply. Designed to have nearly the same dimensions as a conventional railroad tie, the proposed energy harvesting tie can be installed in the same manner as a standard tie on a track. Two rotary electromagnetic energy harvesters are embedded and shielded inside the energy harvesting tie, and the integrated system is capable of generating electricity from the vertical track movement due to passing wheels, in a robust configuration that is suitable for the railroad environment. The integration of the harvesters into a composite tie that has the same appearance of other ties makes less variable to theft and vandalism. A novel ball-screw type mechanical motion half-wave rectification mechanism is adopted in the proposed design to harvest the kinetic energy of the track during its downward motion and rebound upward without any resistance from the harvesters. A simulation study is performed to better understand the system and predict the performance, based on a nonlinear model. Experiments are subsequently carried out in a load frame on a half-tie prototype with both sinusoidal and field-recorded track displacements to measure the amount of power that can be harvested under ideal conditions and actual field conditions. The test results, which agree well with the simulations, indicate a maximum of 78.1% mechanical efficiency is achieved under harmonic excitations. Field-recorded tie displacements yield 16.1–44.5 W of average power depending on the electrical loads, sufficient for powering sensor suite and trackside electronics that could improve track monitoring and safety.

1. Introduction

Well ahead of other modes of transportation, railroads are the most energy-efficient way to transport passengers and move goods, when it comes to limiting greenhouse gas emissions, increasing fuel efficiency, and reducing their carbon footprint. According to *Transportation Statistics Annual Report 2020* [1], the United States has 136,851 miles of track, and its freight rail network is widely considered as the largest freight

* Corresponding author.
E-mail address: panyu@vt.edu (Y. Pan).
[1] Research Scientist, Center for Vehicle Systems and Safety.
[2] Robert E. Hord, Jr. Professor and Director, NSF IUCRC Center for Energy Harvesting Materials and Systems.
[3] J. Bernard Jones Chair and Director, Center for Vehicle Systems and Safety.

https://doi.org/10.1016/j.apenergy.2022.118844
Received 15 September 2021; Received in revised form 10 February 2022; Accepted 24 February 2022

system in the world. However, 75.7% of the total miles of railroad tracks are in rural areas [1] where manual track inspection is not convenient, at times resulting in costly derailments or accident due to unnoticed track issues. The data from the Federal Railroad Administration Office of Safety Analysis indicates that more than 8900 train accidents were reported nationwide in the U.S. from 2016 to 2020, causing 549 casualties [2]. For railroads located in rural areas and tunnels, the electric power is usually inaccessible. Traditional trackside electrical auxiliary devices like signal lights and track switches cannot be economically deployed, as with health monitoring and wireless communication systems that can increase rail operational safety and reliability. Even though batteries can provide power, their environmental unfriendliness and the need for frequent replacement make it not a satisfactory solution. Therefore, finding a reliable and sustainable power source for trackside electrical applications is of utmost importance for the railroad to improve its operational safety and connectivity.

To accommodate the need for usable electricity, researchers around the world have made great efforts in harvesting the available but unused energy from the rail environment, such as thermal, solar, wind, magnetic, and vibration/motion. Gao et al. [3] developed a thermoelectric generator (TEG) using the temperature gradient between the steel rail and the soil below the track foundation, and field tests yielded a maximum average power output of 5.8 mW in the summer. Hao et al. [4] designed a portable solar energy harvesting system with a foldable-wing mechanism for trackside, and they obtained a peak power output of 10.9 W in the lab with a solar simulator. Pan et al. [5] used a portable wind energy harvester for railway tunnels and were able to measure maximum power output of 107.8 mW in wind tunnel testing at wind speeds of 11 m/s. Kuang et al. [6] designed and optimized a magnetic field energy harvester to scavenge energy from AC traction return current in electrified railways. Their laboratory testing resulted in an average power output of 1.6–5.1 W when the developed harvester was placed at 190–45 mm from a track carrying 520 A at 50 Hz. Although the mentioned technologies are affected by temperate gradient, radiation intensity, wind speed, and track type, they provide possible solutions for converting unused trackside energy into useable electrical power under certain circumstances.

During the past decade, energy harvesting from track vibration and deflection has received increased attention, not only because it is independent of the ambient conditions but also due to its vast energy potentials. The frequency and amplitude of track deflections induced by wheel load vary from 1 to 10 Hz and 0.4–12 mm, depending on the train's load, speeds, and bogie distance, as well as the track structure and conditions [7–10]. Piezoelectric materials are among popular approaches for harvesting the rail's vibration energy, and their rail application has been investigated by several researchers. Wischke et al. [11] designed a piezoelectric energy harvester supported by two solid-state hinges with a seismic mass in the middle, and field testing yielded an average scavenged energy of 395 μJ per train when the harvester was mounted on a rail tie in a tunnel. Pourghodrat et al. [12] attached a piezoelectric element to the bottom of a rail and used the rail longitudinal strain to harvest an average power of 53 μW for a train traveling at 24 km/h. Cahill et al. [13] developed three-dimensional finite element models for piezoelectric energy harvesters that can be adhered to the railway bridges. Their numerical simulation showed 588 μW and 307 μW for PZT and PVDF piezo materials at train speed of 120 km/h, respectively. Gao et al. [14] proposed a rail-borne energy harvester that consists of a PZT film with a tip mass, clamped at the bottom of the rail. Their laboratory evaluation indicated an instantaneous peak power of 4.9 mW when a track segment was excited at 5–7 Hz with excitation force of 140 kN. Overall, due to the high impedance of the piezoelectric materials, their output power is fairly low and can only supply sensor networks with extremely low power demands.

Other than the piezoelectric energy harvesters, researchers have also developed track vibration energy harvesters by using linear electromagnetic elements. Pourghodrat and Nelson et al. [12] developed an inductive voice coil device to generate electricity from rail deflection. They achieved an average power output of 4 mW for an empty rail car at 18 km/h, and 12 mW for a loaded coal car at 21 km/h. Using the linear electromagnetic-induction technology, Gao et al. [15] developed one resonant harvester and one magnetic-floating harvester, which are suitable for mounting to the rail base and web, respectively. In their bench testing, a peak power of 119 mW was achieved with 1.2 mm vibration amplitude at 6 Hz for the resonant harvester, and the magnetic-floating harvester yielded 49.2 mW with similar excitations. Later, Sun et al. [16] improved the design of the magnetic-floating energy harvester with a triple-repellent configuration. Their shaker testing showed that the improved harvester has a broader band of power generation and could potentially be used for in-situ inspection of moderate to severe rail corrugation. Hou et al. [17] proposed a linear energy harvester that consists of a mass block, springs, two permanent magnets, and coils, to power strain sensors for railway bridge health monitoring. Their numerical simulations suggested an average power of 0.6 W with a 23 mm displacement input at its resonant frequency. Although linear electromagnetic harvesters significantly increase the piezoelectric harvesters' sub- milliwatts of power to tens or hundreds of milliwatts, their capability is still limited to powering low-power sensors. The root cause of this insufficient power is that the input speed of the track vibration is relatively low, therefore the mechanical input power and the electrical power output both remain inadequate.

In recent years, rotary electromagnetic energy harvesters have been studied as a possible solution to bridge the gap between energy needs and system output because of their greater efficiency and potential for increased power output. The convenient implementation of speed-increasing drivetrains and rotary electromagnetic generators have proven to be the enabling elements. Gopinath [18] and Wang et al. [19] developed a railway track energy harvester with a mechanical motion (full-wave) rectification (MMR) mechanism that can convert the bidirectional track motion into unidirectional rotation of electromagnetic generator through three shafts, three spur gears, a pair of rack and pinion, and two roller clutches. The laboratory experimental results showed a harvested average power of 1.0–1.4 W under 28 mm/second RMS velocity. Meanwhile, Pourghodrat et al. [12,20] independently proposed and tested a different three-shaft MMR track energy harvester that generated 0.19 W and 4.24 W average power in the lab under simulated unloaded and loaded train conditions at 88.5 km/h, respectively. Subsequently, Zhang et al. [21] developed a similar rack pinion based rail energy harvester with a motion rectification mechanism and achieved 55% efficiency in bench testing. To reduce the bearing frictions and gear/shaft misalignments power losses, Wang and Lin et al. [22,23] simplified the overall structure to a single-shaft design with two pairs of racks and pinions. They achieved an increased mechanical power conversion efficiency of up to 74% and proved the updated design with MMR mechanism has the potential to provide more than 10 W of power. The abovementioned bidirectional railway track energy harvesters all require a physical anchor to obtain the relative motion between the input rack and pinion; however, this is difficult for track implementation from the safety and environment perspective. As such, Lin et al. [24] proposed a new anchorless rack-pinion based MMR track energy harvester by incorporating preloaded reset springs that counteract the harvester force during track rebound (i.e., the upward motion). Field testing at the Transportation Technology Center (TTC) in Pueblo, Colorado, demonstrated an average power output of 6.9 W for a freight train traveling at 64 km/h (40 mph) on a ballasted track. Later, to reduce the inherent rack and pinion backlash, a new ball-screw type anchorless MMR harvester was developed for a metro rail with smaller deflections [25]. Field testing resulted in an average power of 2.2 W for an empty metro traveled at 30 km/h, and simulation studies indicated that the harvester does not affect the track dynamics.

Overall, energy harvesters with rotary electromagnetic generators exhibit good power output performance, as compared with other alternatives. However, three main challenges or potential deficiencies

remain. First, the existing rail energy harvesters are directly exposed to the harsh railroad environment and easily prone to damage, theft, or vandalism. Second, the installation and operation of current rail harvesters can impede track regular maintenance, such as ballast tamping, and may bring safety concerns to railroads if unnoticed. Third, the power generation and system reliability of the existing anchorless track energy harvesters are significantly constrained by the reset spring stiffness, as indicated in [24,25], and sufficient spring loads are usually unachievable in the limited height that the railroad can accommodate.

This study aims at reducing or eliminating the shortcomings of the MMR track harvesters by offering a novel ball-screw based mechanism that converts the compression motion into rotation of generator but freewheels in the rebound, referred to as mechanical motion half-wave rectification (MMHR). An MMHR based energy harvesting tie that has nearly the same dimensions as a conventional tie and can be installed readily using the accepted maintenance of way practices, is proposed. Compared with bidirectional harvesters, the MMHR energy harvesting tie harvests the track kinetic energy during its downward movement only. Hence, the concern with an inadequate spring load is eliminated. A nonlinear model is established to analyze the dynamic characteristics of the system. The simulations are performed to better understand the dynamics of the half-wave rectification mechanism and predict its performance. Experiments are subsequently conducted on a half-tie prototype with both sinusoidal and field-recorded track displacements. The test data agree well with the simulation results and shows a maximum of 78.1% mechanical efficiency for harmonic excitations. Field-recorded tie displacement tests indicate the fabricated half-tie prototype is able to generate 16.1–44.5 W of average power from a single rail, depending on the electrical loads of the harvester. A full-size prototype is expected to double the power generation.

The remainder of the paper is organized as follows. Section 2 presents the design of the proposed energy harvesting tie and its working principles. Section 3 establishes the system dynamic model and performs a simulation study. Section 4 discusses the experimental testing of a fabricated half-tie prototype, and Section 5 provides the concluding remarks.

2. Design and working principle

Railroad track deflects vertically due to the moving wheel-rail contact forces. Despite the amplitude is relatively small, the wheel-pass induced track deflection under the high tonnage of the trainload contains a vast amount of energy that can be harvested and utilized [23]. The proposed energy harvesting tie, shown in Fig. 1a, is designed to have nearly the same dimensions as a conventional railroad tie so that it can be conveniently installed and maintained in the same manner as a standard tie. The U.S. Federal Railroad Administration (FRA) regulates that a minimum of 12 effective ties are required for U.S. Class 4 and 5 tracks in each 39-foot (12-meter) segment for safe operation [26]. Commonly, an average of 19–24 ties are installed on a 39-ft segment, providing redundancy for the minimum number of required ties [27,28]. Therefore, replacing a conventional tie with an energy-harvesting tie would keep the track in compliance with the FRA rules.

The tie accommodates two electromagnetic energy harvesters housed in it, which are capable of generating power when a train passes over it. Using the tie as housing protects the harvesters from damage, theft, and vandalism. Through a unique and efficient motion transmission design, the tie can provide tens-of-watt average power output, sufficient for serving as a powering/charging station for wayside sensors and electrical devices, some of which are shown in Fig. 1b.

2.1. Tie design

Fig. 2 provides the design details of the energy harvesting tie. The tie consists of a standard tie with machined spaces for two electromagnetic harvesters and four preloaded coil springs, and a tie box that provides the base support. The energy harvesters are accommodated inside the cavities of the tie, being protected from the harsh railroad environment. As indicated in Fig. 1a and Fig. 2, the harvesters are rigidly connected to the modified tie from the top and the tie box from the bottom. Standard tie plates, clips, and fasteners are used to clamp the rail and the energy harvesting tie together. The relative movement between the tie and tie box causes high speed rotation of the generator, producing energy in the range of tens of Watts. The bending rails and springs return the tie to its undeflected position when not under the direct wheel load. The tie can be used on both ballasted and unballasted tracks, although we anticipate that the ballasted tracks would yield more energy because of their larger vertical deflections due to heavier wheel loads.

The embedded electromagnetic harvester consists of a back-driven ball screw, an enclosed gearbox with a pair of bevel gears, an output shaft with a one-way clutch, and an electromagnetic generator with a speed-increasing gearhead, as illustrated in Fig. 2b. The top casing of the enclosed gearbox, referred to as casing 1, is rigidly connected to the tie by fasteners. The U-shaped nut adapter that is rigidly connected to the ball nut is bolted on the tie box base plate. The energy harvesting tie rests on tamped ballast (on a ballasted track) or subgrade (on a ballastless track). With the four preloaded springs, the tie box can be regarded as relatively stationary. The tie follows the rail deflection, which causes the casings and ball screw to move up and down vertically while the ball nut attached to the tie box remains stationary. The relative reciprocating linear motion between the tie and tie box is transformed into a bidirectional rotation of the ball screw shaft, which rotates the generator's shaft through a gearbox.

The gearbox primarily includes a pair of bevel gears, two thrust bearings, two angular contact bearings, and three pieces of outer casings. The supporting structure, referred to as bearing casing in Fig. 2b, holds another angular contact bearing to support the ball screw shaft from the bottom. The bidirectional rotating screw shaft drives the bevel gear pair, and subsequently, the output shaft rotates in two directions. Instead of being integrated with the large bevel gear, the one-way clutch

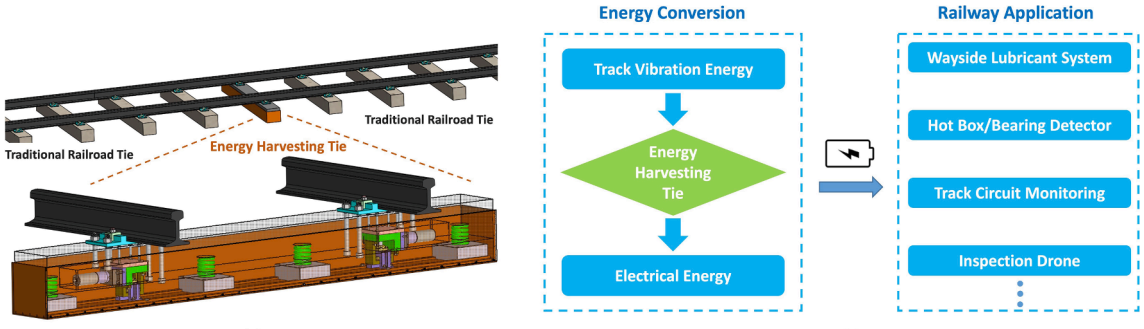

Fig. 1. (a) Design overview of energy harvesting tie; (b) various railway applications can be powered by energy harvesting tie to improve rail safety and connectivity.

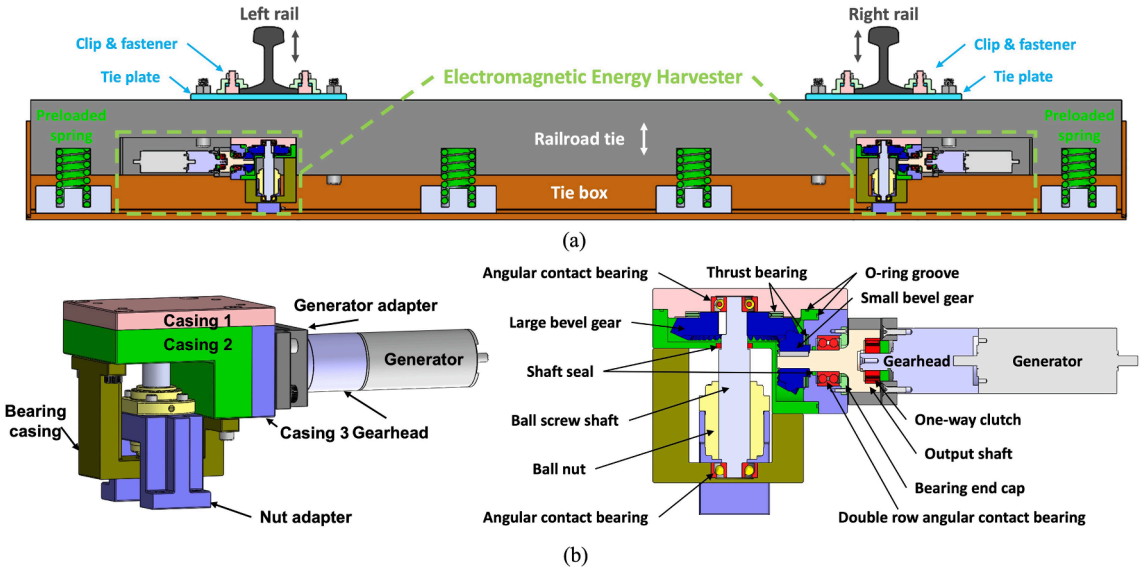

Fig. 2. Energy harvesting tie design: (a) cross-sectional view as installed on a track; (b) embedded electromagnetic energy harvester.

is placed at the output end so that the torque requirement and associated friction can be reduced. The outer ring of the clutch is press-fitted into the bore of the output shaft and its inner ring has a keyway that can transmit torque from the shaft to the gearhead in one direction. Consequently, the electromagnetic generator can be driven unidirectionally at a relatively high speed. The O-ring grooves and shaft seals are designed to seal the inside the gearbox.

2.2. Working principle of the embedded electromagnetic energy harvester

Fig. 3 demonstrates the working principle/motion transmission of the embedded electromagnetic energy harvester. The red arrows represent the direction of movement when a wheel approaches , while the green arrows show the return to the undeflected position. Under the force of a passing wheel, the tie moves downward with a small amplitude, and the harvester sandwiched in between the tie and tie box is compressed. This low-speed linear compression is translated into the rotation of the ball screw shaft and the bevel gear pair, rotating the output shaft at a higher speed. The engaged one-way clutch transmits torque and motion to the gearhead's shaft, driving the generator at a relatively high speed to generate electrical power.

In rebound, the bending rails and preloaded springs return the tie to the undeflected position, driving the ball screw shaft, bevel gears, and output shaft to rotate in the opposite direction. The one-way clutch is disengaged from the gearhead's shaft in the rebound, disconnecting the generator from the gearbox. The generator can continue spinning with its momentum and electrical damping but receives no additional torque until the next compression cycle of the tie.

As opposed to the previously developed railroad energy harvesters [23–25] that typically harvest energy from bidirectional track motions, the proposed energy harvesting tie uses a single one-way clutch that allows harvesting energy in compression cycle only. This is analogous to a half-wave electrical rectifier in the electrical domain. Hence, we will refer to it as "mechanical motion half-wave rectification" (MMHR). This MMHR mechanism enables avoiding the demanding requirement of huge spring loads in rebound cycles of bidirectional track harvesters [25]. Its design and implementation not only eliminate the large preload and installation challenges with past designs but also creates more room and flexibility for optimizing the performance.

Table 1 lists the main parameters of the prototyped energy harvesting tie.

3. System dynamics and modeling

3.1. Three-phase AC generator dynamic model

As mentioned earlier, two three-phase AC generators are integrated into the energy harvesting tie. The induced phase voltage of a three-phase AC generator connected with Wye resistive loading has been discussed and analyzed in [24]. The power dissipated in the resistive

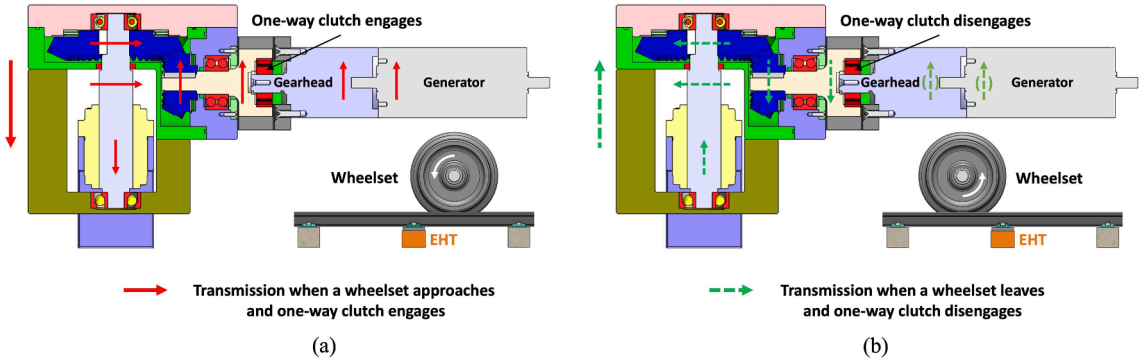

Fig. 3. Downward track motion is transmitted and converted into generator rotation: (a) the red arrows show the direcction of motion in response to track defelectoin due to a passing wheel; (b) the green arrows represent the motion in rebound to return to undeflected position. (For interpretation of the references to color in this figure legend, the reader is referred to the web version of this article.)

Table 1
Parameters of the prototyped energy harvesting tie.

Parameters	Value	Description	Parameters	Value	Description
d_s	25.4 mm	Ball screw stroke	J_{ge}	0.264 kgcm^2	Generator rotor inertia
d_m	25 mm	Ball screw shaft diameter	r_b	2	Bevel gear transmission ratio
l	25 mm	Ball screw lead	r_g	19	Gearhead amplification ratio
J_{bs}	0.43 kgcm^2	Ball screw shaft inertia	k_s	37 kN/m	Coil spring stiffness
J_{lb}	4.73 kgcm^2	Large bevel gear inertia	n_p	8	Generator's number of pole pairs
J_{sb}	0.36 kgcm^2	Small bevel gear inertia	k_e	0.072 V/rads	Generator voltage constant
J_{os}	1.09 kgcm^2	Output shaft inertia	k_t	0.072 Nm/A	Generator torque constant
J_{gh}	0.0095 kgcm^2	Gearhead inertia	R_i	0.12 Ω	Generator phase resistance

loads can be considered as the electrical power output from the energy harvester.

The resistive torque T_{ge_d} induced by the electrical damping of the three-phase AC generator can be expressed as

$$T_{ge\_d} = \frac{3k_t k_e}{2(R_i + R_e)}\omega_{ge} = c_{ge}\omega_{ge} \tag{1}$$

where k_t is the generator torque constant, k_e is the generator voltage constant, R_i is the internal generator phase resistance, and R_e is the external phase resistive load. ω_{ge} represents the angular velocity of the generator's rotor shaft, and $c_{ge} = \frac{3k_t k_e}{2(R_i+R_e)}$ is the equivalent damping coefficient of the generator. From the above equation, it should be noted that the resistive damping torque can be tuned by varying the connected external phase load resistance. At a given angular velocity of the generator, smaller external phase loads result in a larger damping torque T_{ge_d}, which implies a higher capability of converting the mechanical power to electrical power.

The resistive torque T_{ge_i} induced by the rotational inertia of the generator's rotor can be expressed as

$$T_{ge\_i} = J_{ge}\dot{\omega}_{ge} \tag{2}$$

where J_{ge} is the generator rotor inertia, and $\dot{\omega}_{ge}$ represents the angular acceleration of the generator.

Therefore, the total driving torque for the electromagnetic generator is the sum of the inertia torque T_{ge_i} and damping torque T_{ge_d}, and can be expressed as

$$T_{ge} = T_{ge\_i} + T_{ge\_d} = J_{ge}\dot{\omega}_{ge} + \frac{3k_t k_e}{2(R_i + R_e)}\omega_{ge} \tag{3}$$

3.2. Energy harvesting tie dynamic model

The proposed energy harvesting tie incorporates two embedded electromagnetic energy harvesters to harvest the kinetic energy of both left and right rails and is symmetrical about the centerline of the track. For simplicity, only half of the energy harvesting tie with a single displacement input is considered in the model. Fig. 4 shows the schematic diagrams of a half energy harvesting tie during its operation at two different modes: engagement mode and disengagement mode. Engagement mode represents that the integrated one-way clutch engages with the generator gearhead. The dynamics can be described by a single-degree-of-freedom system. Disengagement mode stands for that the one-way clutch disengages/separates with the generator gearhead. This mode can be modeled as two subsystems with different dynamic characteristics.

Let us denote the vertical displacement and velocity of the tie as x and $\dot{x}$, and the angular velocity of the ball screw shaft, large bevel gear, small bevel gear, output shaft, gearhead, and generator as ω_{bs}, ω_{lb}, ω_{sb}, ω_{os}, ω_{gh}, and ω_{ge}, respectively. Then, the rotation of the transmission driveline and electromagnetic generator can be described by:

$$\frac{2\pi}{l}\dot{x} = \omega_{bs} = \omega_{lb} = \frac{1}{r_b}\omega_{sb} = \frac{1}{r_b}\omega_{os} \tag{4}$$

$$\omega_{ge} = r_g\omega_{gh} \tag{5}$$

where l is the lead length of ball screw, r_b is the bevel gear transmission ratio, and r_g is the gearhead amplification ratio.

3.2.1. Compression cycle

When the tie moves down (i.e., $\dot{x} < 0$), the system can be in engagement mode or disengagement mode, depending on the rotational speed of the one-way clutch's outer and inner rings (i.e., the speed of the output shaft ω_{os} and generator gearhead ω_{gh}). If the outer ring's speed is lower than the inner ring, the generator disengages with the gearbox, otherwise, it engages. In other words,

- When $\omega_{os} = \frac{2\pi r_b}{l}\dot{x} = \omega_{gh}$, the one-way clutch engages and transmits torque and motion
- When $\left|\omega_{os} = \frac{2\pi r_b}{l}\dot{x}\right| < |\omega_{gh}|$, the one-way clutch disengages with the gearhead and generator, and the generator continues rotating due to inertia and slows down due to electrical damping until it completely stops or being engaged again

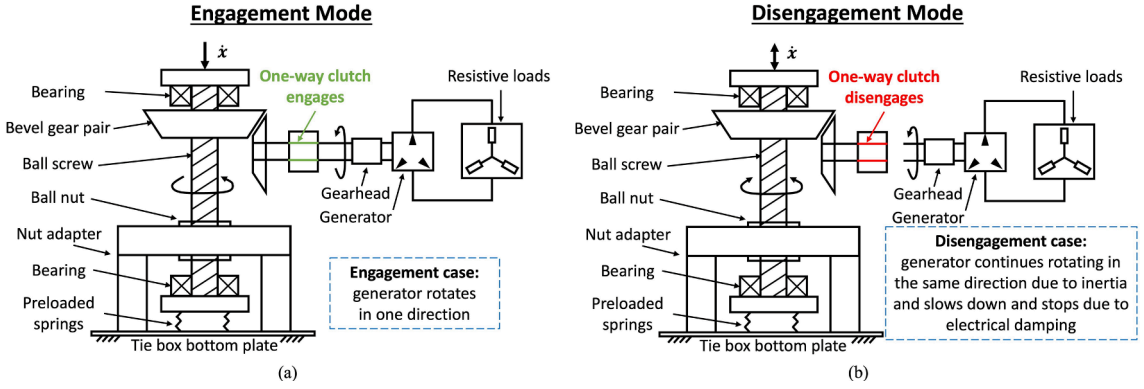

Fig. 4. Schematic diagram of the energy harvesting tie model for single rail: (a) engagement mode; (b) disengagement mode.

More specifically, as shown in Fig. 4a, the ball nut and the nut adapter are considered to be stationary, then the ball screw shaft moves downward and spins clockwise (from the bottom view) at the same time, driving the bevel gear pair and the output shaft successively through key connections and gear meshing. When the rotational speed of the small bevel gear ω_{sb} (or output shaft ω_{os}) equals the generator's gearhead ω_{gh}, the embedded one-way clutch's inner ring engages with the outer ring through a series of sprags in between; hence torque and motion are transmitted from the ball screw to the electromagnetic generator.

Therefore, the resistive damping force between the two terminals of the energy harvester can be expressed as

$$F_d = \frac{2\pi r_b r_g}{l} T_{ge\_d} = \frac{6\pi^2 k_t k_e r_b^2 r_g^2}{l^2 (R_i + R_e)} \dot{x} = c_e \dot{x} \tag{6}$$

where $c_e = \frac{6\pi^2 r_b{}^2 r_g{}^2 k_t k_e}{l^2 (R_i + R_e)}$ represents the system's equivalent damping coefficient.

Since the electromagnetic energy harvester can be considered as a single-degrefe-of-freedom system in the engagement mode, using the energy method, the kinetic energy of the system can be expressed as

$$T_{kinetic} = \frac{1}{2} m_e \dot{x}^2 = \sum_1^n T_{k_i} = \frac{1}{2} J_{bs} \omega_{bs}^2 + \frac{1}{2} J_{lb} \omega_{lb}^2 + \frac{1}{2} J_{sb} \omega_{sb}^2 + \frac{1}{2} J_{os} \omega_{os}^2 + \frac{1}{2} J_{gh} \omega_{gh}^2 + \frac{1}{2} J_{ge} \omega_{ge}^2 \tag{7}$$

where m_e stands for the equivalent mass of the system, and J_{bs}, J_{lb}, J_{sb}, J_{os}, J_{gh}, and J_{ge} represent the moment of inertia of the ball screw shaft, large bevel gear, small bevel gear, output shaft, gearhead, and generator, respectively. Substituting Eqs. (4) and (5), and $\omega_{gh} = \omega_{sb}$, into Eq. (7), the equivalent mass of the energy harvester m_e in the engagement mode can be derived as

$$m_e = \frac{4\pi^2}{l^2} (J_{bs} + J_{lb} + r_b^2 J_{sb} + r_b^2 J_{os} + r_b^2 J_{gh} + r_b^2 r_g^2 J_{ge}) \approx \frac{4\pi^2}{l^2} r_b^2 r_g^2 J_{ge} \tag{8}$$

where the contribution of $(J_{bs} + J_{lb} + r_b^2 J_{sb} + r_b^2 J_{os} + r_b^2 J_{gh})$ is far less than that of $r_b^2 r_g^2 J_{ge}$, as can be perceived and calculated from Table 1. Therefore, the equivalent mass of the system during the engagement is predominantly dominated by the moment of inertia of the electromagnetic generator, J_{ge}, if the gear ratios and the lead of the ball screw are fixed.

Considering the preloaded springs in the half-tie model, the total resistive force between the two terminals during engagement can be expressed as

$$F_{engage}^{down} = m_e \ddot{x} + c_e \dot{x} + 2k(x + \delta_0) = \frac{4\pi^2}{l^2} r_b^2 r_g^2 J_{ge} \ddot{x} + \frac{6\pi^2 k_t k_e r_b^2 r_g^2}{l^2 (R_i + R_e)} \dot{x} + 2k_s (x + \delta_0) \tag{9}$$

where k_s represents the coil spring stiffness and δ_0 is the initial compression length of the springs. Equation (9) suggests that the energy harvesting tie can be regarded as an inerter in parallel with preloaded springs and a tunable damper. By adjusting the load resistance R_e, the equivalent damping of the system can be tuned to the desired values for the application's power need.

The phase voltage of the AC generator in Wye configuration can also be derived through motion transmission relationship as

$$V_{k\,engage}^{down} = \frac{2\pi r_b r_g k_e}{l} sin\left(\int_0^t \omega_e dt + \frac{2k}{3}\pi \right) \dot{x} \tag{10}$$

where $k = 0, 1, 2$, representing the three phases of the AC generator, respectively.

The system can also be in disengagement mode when the tie moves downward if the absolute angular velocity of the output shaft becomes smaller than the gearhead's. In such a condition, as shown in Fig. 4b, the inner ring of the one-way clutch embedded in the output shaft disengages from the outer ring and stops transmitting torque from the ball screw to the generator. Hence, the generator can continue rotating due to its momentum while slowing down because of the electrical damping and losses until the next engagement.

The total resistive force of the system's two terminals and the phase voltage generated during disengagement when the tie moves down can be expressed as

$$F_{disengage}^{down} = \frac{4\pi^2}{l^2} \left(J_{bs} + J_{lb} + r_b^2 J_{sb} + r_b^2 J_{os} + r_b^2 J_{gh} \right) \ddot{x} + 2k(x + \delta_0) \approx 2k(x + \delta_0) \tag{11}$$

$$V_{k\,disengage}^{down} = \dot{\theta}_0 sin\left(\int_0^t \omega_e dt + \frac{2k}{3}\pi \right) e^{-\frac{c_{ge}}{J_{ge}}(t - t_0)} = \dot{\theta}_0 sin\left(\int_0^t \omega_e dt + \frac{2k}{3}\pi \right) e^{-\frac{3k_t k_e}{2J_{ge}(R_i + R_e)}(t - t_0)} \tag{12}$$

where $\dot{\theta}_0$ and t_0 are the instantaneous angular velocity of the generator and moment, respectively, when disengagement occurs.

3.2.2. Rebound cycle

When the tie moves upwards, $\dot{x} > 0$ (i.e., the rebound cycle), the bevel gear pair, the output shaft, and the outer ring of the one-way clutch will rotate in the opposite direction, causing the generator to disengage from the drivetrain, as illustrated in Fig. 4b. Hence, for the rebound cycle, the total resistive force and generated voltage are simplified to:

$$F^{up} \approx 2k(x + \delta_0) \tag{13}$$

$$V_k^{up} = \dot{\theta}_0 sin\left(\int_0^t \omega_e dt + \frac{2k}{3}\pi \right) e^{-\frac{c_{ge}}{J_{ge}}(t - t_0)} = \dot{\theta}_0 sin\left(\int_0^t \omega_e dt + \frac{2k}{3}\pi \right) e^{-\frac{3k_t k_e}{2J_{ge}(R_i + R_e)}(t - t_0)} \tag{14}$$

where $\dot{\theta}_0$ and t_0 are the instantaneous angular velocity of the generator and time, respectively, at the moment that the disengagement occurs during the previous compression cycle.

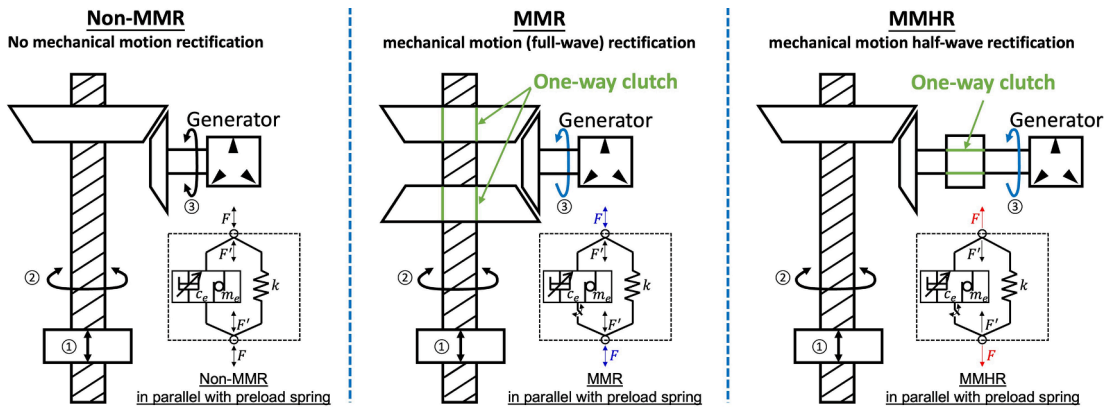

Fig. 5. Ball-screw based Non-MMR, MMR, and MMHR mechanisms, and their models coupled with preloaded return spring. The motion flow starts from the relative linear reciprocal motion ① between the ball nut and screw shaft to the bidirectional screw shaft rotation ②, and eventually delivers to be the generator rotation ③.

3.3. Comparison between MMHR harvester and MMR/Non-MMR harvesters

Two different motion transmission mechanisms have been widely used in electromagnetic energy harvesters, MMR mechanism and Non-MMR mechanism. "MMR" stands for mechanical motion (full-wave) rectification, which is a unique mechanism that translates a bidirectional linear motion into a unidirectional rotation with the help of two one-way clutches. In contrast, in Non-MMR harvesters a bidirectional linear motion yields a bidirectional rotation, without any rectification. The comparison between MMR and Non-MMR has been investigated in [29,30], and the higher power output and conversion efficiency of MMR harvesters have been well recognized.

Different from the above two mechanisms, the proposed design of energy harvesting tie adopts a novel mechanism that transfers a single-direction motion into a unidirectional rotation of the generator. Here, this distinct mechanism, analogous to the electrical half-wave rectifier, is referred to as "mechanical motion half-wave rectification," or MMHR. The non-MMR, MMR, and MMHR have been shown schematically in Fig. 5. The inset figure for each includes the dynamic model for each configuration, coupled with the preloaded return spring.

As shown in Fig. 5, Non-MMR energy harvesters can be modeled as a linear inerter in parallel with a tunable damper, while the MMR system, due to the switching of engagement and disengagement, can be modeled as a nonlinear inerter damper. The MMHR configuration shares similar model elements with MMR but possesses different switching time points, resulting in distinctive system dynamics. It has a one-way clutch that can be engaged to transmit torque in the compression cycle but does not have a second clutch to do the same in the rebound cycle, unlike MMR harvesters.

The results of dynamic simulations (coupled with preload springs) for a sinusoidal displacement are presented in Fig. 6 for two different electrical resistances. The simulation parameters of the Non-MMR and MMR harvesters are chosen the same as the prototyped design with MMHR mechanism, as listed in Table 1.

The linear displacement and velocity inputs have been shown on the plot, and the theoretical angular velocity of the generator for all three systems with different transmission mechanisms are also presented. The force plots represent the force applied to the tie box by the harvester. A positive force indicates the system requires additional spring load to

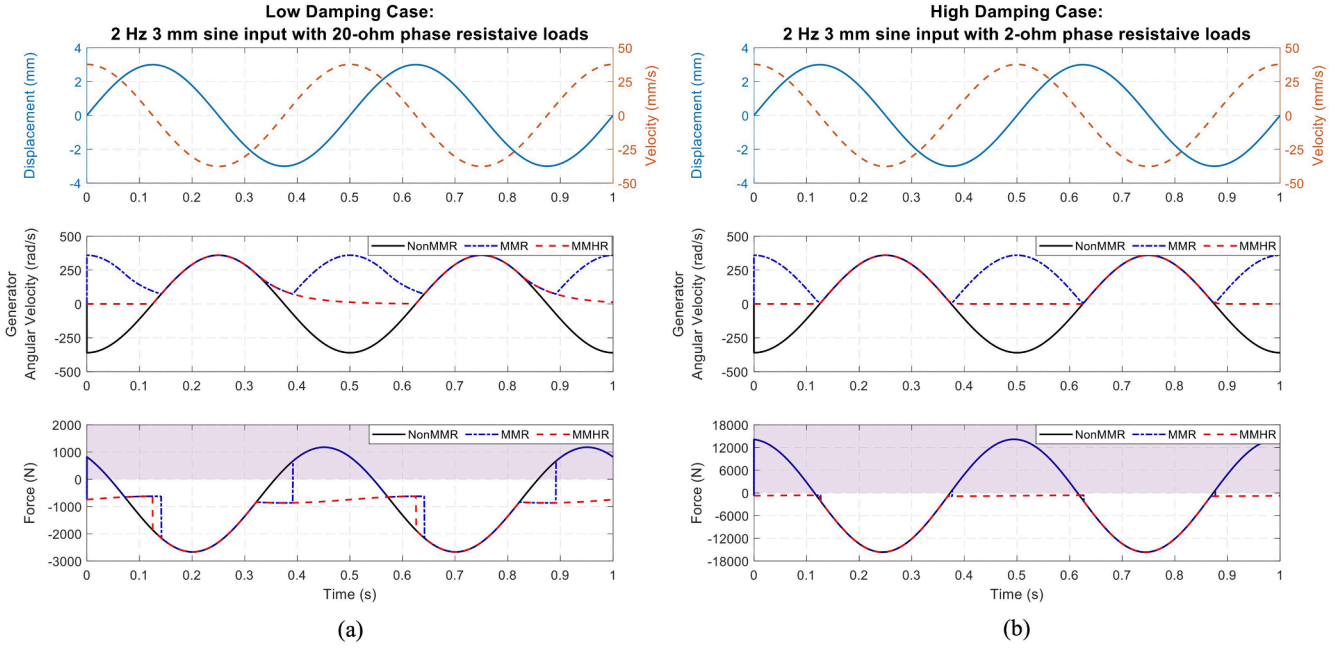

Fig. 6. Dynamic simulation for Non-MMR, MMR, and MMHR harvesters under a sinusoidal displacemnet input of 2 Hz and 3 mm with differnet electrical loads; (a) low damping case (20 Ω); (b) high damping case (2 Ω).

keep the tie box stationary so as to obtain the relative displacement input, while a negative force means that the tie box is supported by the subgrade and the system is functioning as intended. The generated voltage is proportional to the angular velocity, so it can be noted that Non-MMR and MMR harvesters may generate more power in both low and high damping cases if they are able to operate properly. However, with a spring preload of 750 N, the harvester with Non-MMR and MMR mechanism produces both positive and negative forces during the operation. The positive force in the shaded area in Fig. 6 would lift and separate the harvesters from the supporting ballast or subgrade. Specifically, take the high damping case shown in Fig. 6b as an example; both Non-MMR and MMR harvesters yield more than 15,000 N maximum positive force, which means that an additional 15,000 N spring load is needed to counteract the positive force. Otherwise, the harvester would float and lose terminal support, no longer generating power as desired. This separation would also bring impact forces when the systems reunite with the bottom support during the next cycles of downward motion, accelerating component wear and diminishing system reliability. Theoretically, this problem could be avoided by increasing the spring preloads, stiffness, or both, but it proves to be difficult in practice due to height limitations in railroad.

The MMHR design inherently and fundamentally solves this problem by eliminating the need for large spring force in the rebound cycle since it only harvests kinetic energy during the compression cycle. As shown both in Fig. 6a and b, with a 750 N spring preload–deemed to be a suitable preload for easy installation–the MMHR forces are always negative (compressive), indicating the system is firmly supported by the track subgrade all the time, resolving the reliability issues with past designs, and ensuring MMHR energy harvesting tie a robust transmission and stable electrical power generation. Compared with the conventional rail ties that have very large vertical stiffness and transfer the huge wheel load to the track bed, since the MMHR harvester allows system's vertical compression, the proposed energy harvesting tie transfers far less load and therefore has little effect on the supporting track bed.

3.4. Simulation with different resistive electrical loads

Fig. 7 shows the simulated total resistive force and phase voltage for a 2 Hz and 3 mm sinusoidal input with different load resistances. The total spring preload is set to 750 N, which is intended to keep the tie box stationary on the ballast or subgrade and assist the tie in rebounding when unloaded. Fig. 7a presents the simulated results with 20 Ω phase resistance. The total average power is calculated as the time integration of instantaneous phase power in all three phases. An average power of 11.4 W is achieved in this 20 Ω case. As previously derived, $c_{ge} = \frac{3k_t k_e}{2(R_i+R_e)}$, and $c_e = \frac{6\pi^2 r_b{}^2 r_g{}^2 k_t k_e}{l^2(R_i+R_e)}$, therefore, a 20 Ω phase resistance would result in a smaller equivalent damping compared to a smaller electrical load. It should be noted that the engagement happens only in the compression cycle (i.e., $\dot{x} < 0$) and the generator continues rotating due to its momentum after disengagement occurs and slows down gradually due to its small electrical damping. In rebound cycle (i.e., $\dot{x} > 0$), the energy harvesting tie is always in disengagement mode.

Fig. 7b demonstrates the simulated results with 2 Ω resistive loadings. Since the generator's internal resistance is as small as 0.12 Ω as listed in Table 1, varying the external resistance from 20 Ω to 2 Ω doesn't affect much on the peak phase voltage across the external loads. The generated average power is 99.2 W in all three phases with 2 Ω resistive loading, which is far higher than with 20 Ω. This is because 2 Ω load resistance would result in much higher damping and therefore, more electrical power is converted from the input mechanical power. It is worth mentioning that 2 Ω is the smallest resistive loading that is selected for both simulations and experiments since a lower one would require external forces that could exceed the mechanical strength of the internal components of the energy harvester, if the input velocity were too high. The figures also suggest that with a smaller resistive loading, the period of engagement increases in the compression cycle, and less electrical power is generated in the disengagement cycle.

Overall, with MMHR mechanism and reset springs, the system only harvests the kinetic energy in the compression cycle but refuses to do so in the rebound cycle. In this way, independent of the equivalent damping of the system, the total force between the two terminals of the harvester is always negative, indicating that the force applied at the bottom end of the system (i.e., tie box) is always pointing downward and the tie box is kept stationary on a tamped ballast bed or subgrade. Therefore, the energy harvesting tie with MMHR mechanism is free from the "insufficient spring force" issue that has existed in the previous railroad energy harvesters [24,25]. More details will be discussed in the following subsection.

4. Lab bench test and analysis

4.1. Test setup

An energy harvesting tie prototype is designed and fabricated. To

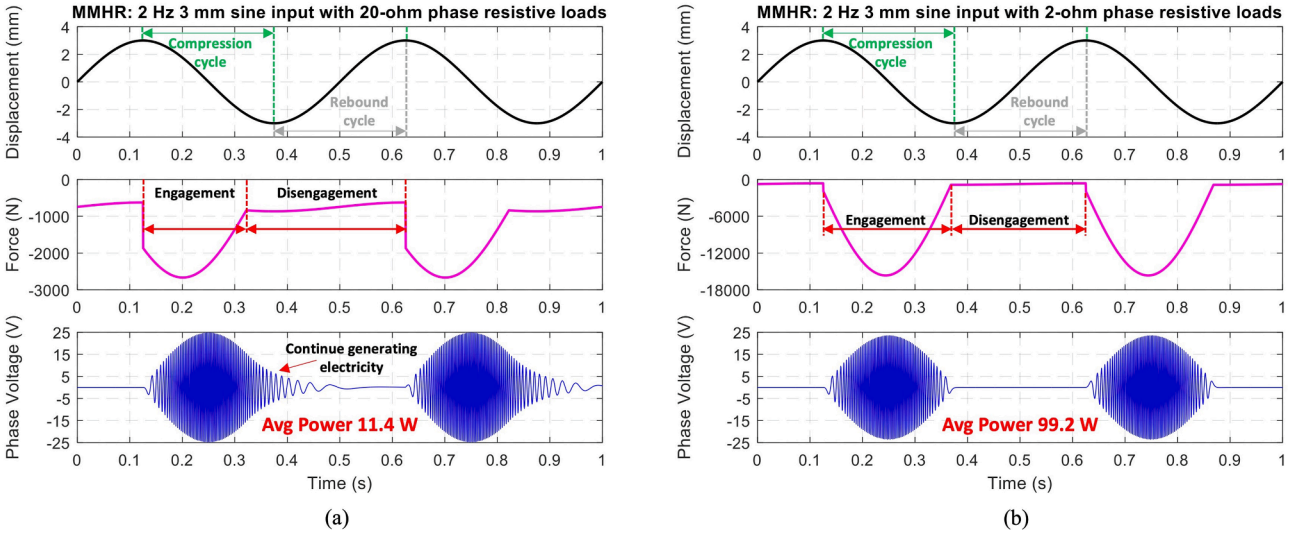

Fig. 7. Simulated system total resistive force and generated phase voltage for 2 Hz 3 mm sinusoidal excitation; (a) with 20 Ω resistive loading; (b) with 2 Ω resistive loading.

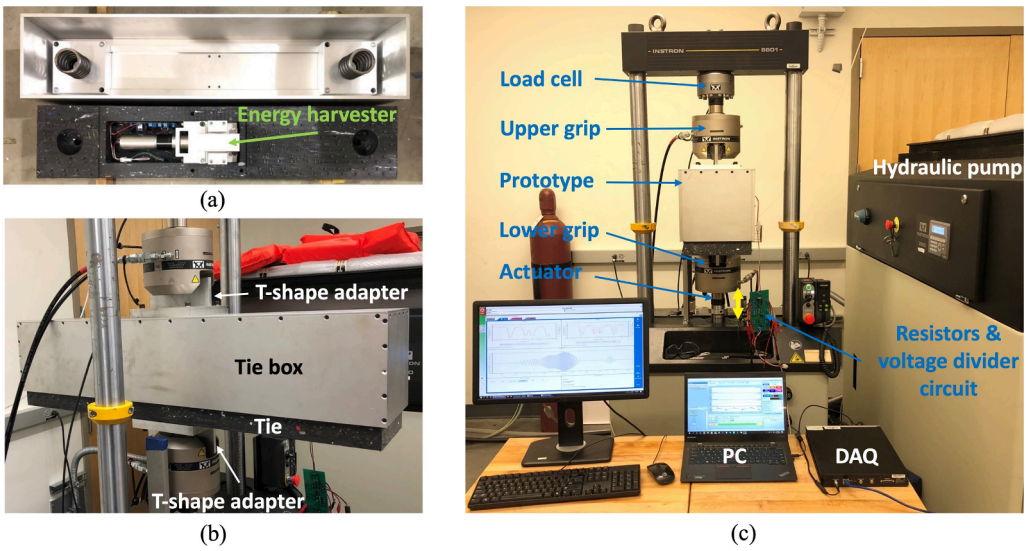

Fig. 8. Test setup for a ½-tie energy harvesting prototype: (a) a single electromagnetic energy harvester is embedded in the ½-length tie; (b) prototype installation in the load frame; (c) the hydraulic load frame and data acquisition system.

better accommodate testing in a load frame, the prototype uses a tie that is about ½ of the length of a full tie and one harvester, as opposed to two that are used in a full-scale energy harvesting tie. As shown in Fig. 8a, the half-tie prototype is comprised of a composite tie, one electromagnetic energy harvester, two reset coil springs, and a scaled tie box. At the top, the harvester is clamped to a fixed crosshead, while the bottom is attached to a controlled hydraulic actuator through T-shaped adapters, as shown in Fig. 8b. In Fig. 8c, the 100 kN load cell that has a resolution of 60 N at the top measures the resulting force from the controlled displacement excitation by the actuator. The testing prototype is installed vertically on the test rig in the reverse direction as installed in the field. The lower grip, driven by the actuator and acting like the deflected rail, provides the displacement excitation. The upper grip is fixed, and the load cell measures the dynamic forces on the tie box. The load cell's sign convention is such that positive measurements indicate tension (separating) loading, while negative measurements indicate compressive loading.

At the start of a test, a preload force of 750 N is applied to the harvester by compressing it by approximately 10 mm. Different external resistive loads are connected to the generator in Wye configuration during the experiment, and the power dissipated on the power resistors is measured to determine the electrical power that the harvester can convert from the mechanical power. A 19:1 three-phase voltage divider is used to scale down the generated voltage to the allowable measuring

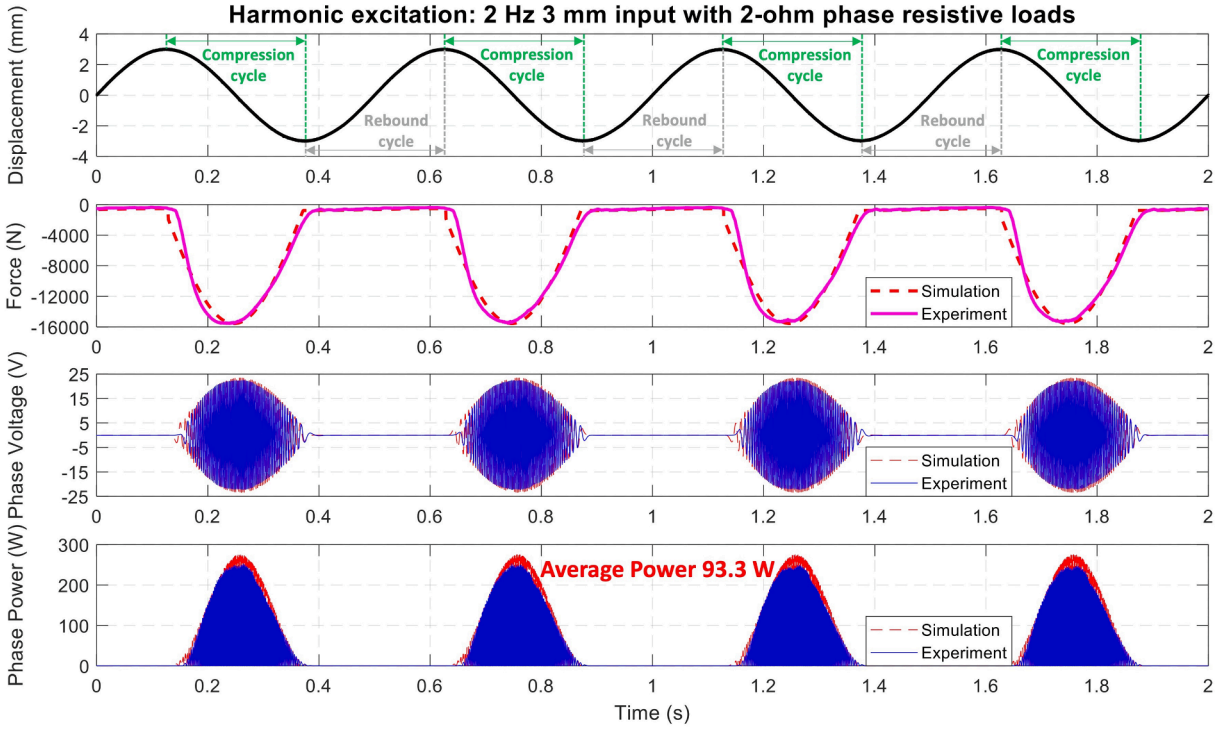

Fig. 9. Measured and simulated force, phase voltage, and phase power with 2 Hz and 3 mm sinusoidal excitation and 2 Ω resistive loadings in Wye configuration. An average power of 93.3 W is achieved.

range for the data acquisition system. The prototype is tested with both sinusoidal and field-measured rail displacements.

4.2. Sinusoidal displacement

A series of experiments with different excitation frequencies, amplitudes, and external resistive loads were performed to evaluate the energy harvesting performance under sinusoidal excitation. During the experiment, the testing prototype starts generating power with 0.2 mm displacement, indicating nearly no dead band in the harvester, signifying the energy harvesting tie has a quite small backlash and is capable of sensing and harvest energy even from tiny vibrations. Fig. 9, as an example of sinusoidal tests, shows the measured displacement, force, and voltage across the resistive load for a 2 Hz and 3 mm input with 2 Ω phase resistive loading. As shown in the displacement subplot, an increasing displacement represents the hydraulic actuator moves downward and the embedded energy harvester is in rebound cycle; while a decreasing displacement denotes the hydraulic actuator moves upward and the harvester in the compression cycle. The solid lines represent the measured force, phase voltage, and calculated phase power, while the dashed lines represent the simulation estimates. As indicated on the plot, the force is always negative, and the testing prototype only harvests the energy in the compression cycle during engagement of the clutch but does not harvest any energy from the extension stroke. An average power of 93.3 W is generated, providing promising results for additional track testing. The test results match well with the simulation results, verifying the effectiveness of the developed dynamic model.

Fig. 10 summarizes the results of the sinusoidal tests under various conditions. Different frequencies and amplitudes emulate various railcar speed and loading conditions. A maximum average power of 147.7 W was achieved under 2 Hz frequency and 4 mm amplitude with 2 Ω resistive loads in the Wye configuration. As we can see from the calculated results, with a given resistive load, the average power increases with increasing input frequency and amplitude due to the higher rotational driven speed of the generator. It is also worth noting that, smaller resistive loading results in larger electrical damping coming from the generator; therefore, with the same excitation input, more mechanical kinetic power can be translated to electrical power when the resistive loads decrease from 8 Ω to 2 Ω.

Mechanical efficiency (η_m), another essential indicator of the harvester's performance, measures how well the harvester converts input work W_{mech}, to electrical output energy E_{elec}, as expressed by Eqs. (15)–(17). As shown by the color bars in Fig. 10, a higher mechanical efficiency is generally obtained with a larger excitation input and a smaller resistive load. The largest η_m (78.1%) is achieved with 2 Hz and 4 mm displacement and 2 Ω resistive loadings, among all the sinusoidal tests.

$$W_{mech} = \int_0^t F(t)\bullet \mathrm{D}(t)\mathrm{d}t \tag{15}$$

$$E_{elec} = 3 \times \int_0^t \left[\left(\frac{V_e(t)}{R_e} \right)^2 (R_i + R_e) \right] dt = \frac{3(R_i + R_e)}{{R_e}^2} \int_0^t V_e(t)^2 dt \tag{16}$$

$$\eta_m = \frac{E_{elec}}{W_{mech}} = \frac{3 \times \int_0^t \frac{(R_i+R_e)V_e(t)^2}{{R_e}^2} dt}{\int_0^t F(t)\bullet D(t) dt} = \frac{3(R_i + R_e) \int_0^t V_e(t)^2 dt}{{R_e}^2 \int_0^t F(t)\bullet D(t) dt} \tag{17}$$

$F(t)$ is the input force measured by the load cell, and $D(t)$ is the input displacement. R_i and R_e are the internal and external phase resistive loads, respectively. $V_e(t)$ is the generated voltage measured across the phase resistive load, R_e.

4.3. Field-measured displacement

Track displacement measurements from field tests with a freight train on a heavy rail traveling at 64 km/h (40 mph) [24] and a metro train traveling on a light rail at 20 km/h (13 mph) and 30 km/h (19 mph) [25] are used for additional evaluation of the prototype harvester performance in the lab. These tests are intended to bring the simulated inputs closer to actual field conditions.

4.3.1. Freight track tie displacement

Fig. 11 shows the experimental results under the recorded tie displacement measurements with 2 Ω resistive loads. This tie displacement was measured by a laser displacement sensor on the High Tonnage Loop (HTL) at the Transportation Technology Center (TTC) in Pueblo, Colorado, with a loaded 27-car freight train at 64 km/h (40 mph) on a ballasted track [24]. Using the recorded displacement as input to the energy harvesting tie yields an average power of 44.5 W in all three phases, demonstrating the half-tie prototype has an excellent capability to harvest tens-of-watt electrical power from a single rail.

The zoomed-in results between 40 and 44 sec in Fig. 11 clearly show how force, phase voltage, and power evolve with the field-recorded tie displacement excitation. The displacement valleys ① through ④ on the zoom-in plot represent the maximum rail deflection/tie movement due to the 1st to 4th passing wheels of a car. The tie movement in compression is represented by decreasing displacements while increasing displacements denote rebound. As indicated, with 2 Ω resistance, the system only harvests mechanical energy and generates electricity in the compression cycle. In rebound, the one-way clutch has been disengaged, and there is no electrical power output. Since the distance between the 2nd and 3rd wheel spans longer in a railcar, the energy harvesting tie can fully rebound between the time it takes for the 2nd and 3rd wheels to pass over it. As explained in Sections 2 and 3, the MMHR harvester only harvests energy in the compression cycle. Therefore, there is a large power output when the 3rd wheel is approaching, but no power output after 2nd wheel leaves. Since the distance between any other two adjacent wheels is relatively short, the rail and tie cannot fully rebound to the unloaded height. This causes the next compression stroke to be fairly small. Therefore, the associated

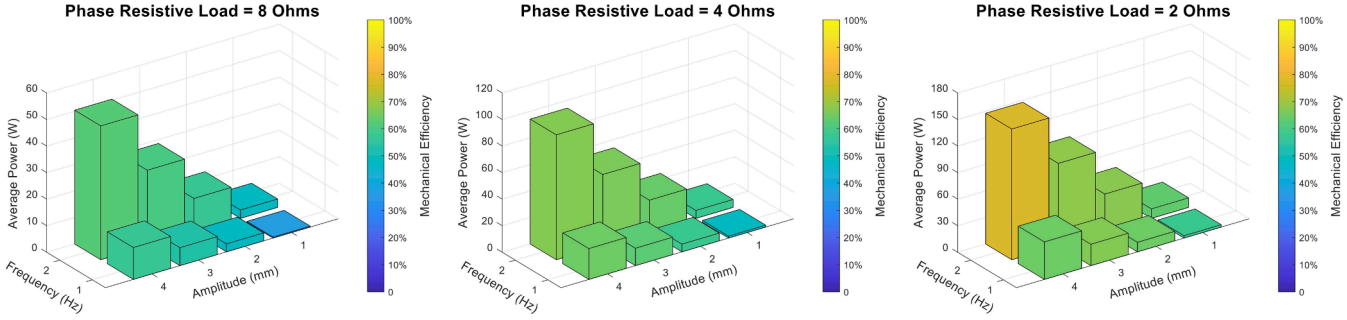

Fig. 10. Average power under sinusoidal excitations with various frequencies, amplitudes, and resistive loads. The color bars represent the mechanical efficiency achieved by the testing prototype.

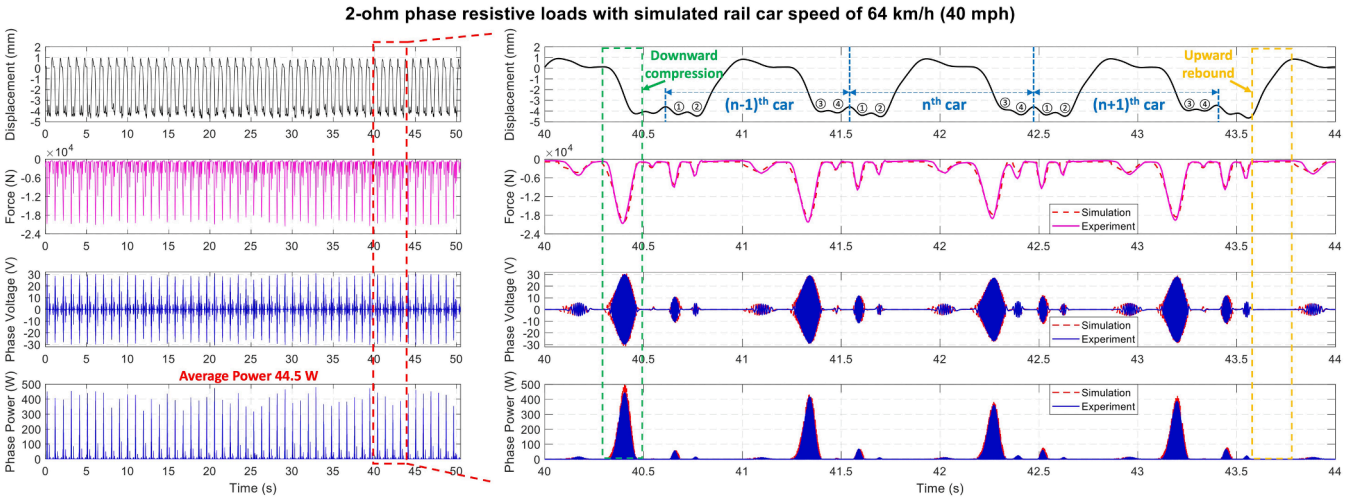

Fig. 11. Half-tie prototype laboratory testing with field-measured tie displacement from a loaded freight train, with 2 Ω Wye resistive loading. An average power of 44.5 W is achieved in three phases. A zoomed-in plot on the right shows the results for t = 40 to 44 sec.

Table 2
Power generation (for a single rail) under recorded tie displacement of a freight rail track (64 km/h) with various loads.

Speed	Resistor		
	8 Ω	4 Ω	2 Ω
64 km/h (40 mph)	16.1 W	27.7 W	44.5 W

power peaks are much lower. The test results match well with the simulation estimates, validating the accuracy of the dynamic model. It is worth noting that the force is always negative, implying that the harvester resists compressive loads and offers little to no resistance in the rebound, in contrast to earlier MMR harvesters that require resisting both compressive and rebounding forces [24,25]. In other words, with this MMHR mechanism, the energy harvesting tie doesn't require a large spring resilience force for keeping the tie box stationary, thereby resolving the spring load and installation challenges of bidirectional harvesting.

Table 2 summarizes the average harvested power for various resistive loads for a single rail. Smaller resistive loads result in larger electrical damping; therefore, more mechanical power can be transferred to electrical power from 8 Ω to 2 Ω. With all resistive loads, the harvester's output is more than 15 Watts, a significant increase over past harvesters. Through adjusting the resistive load, the power output can be adjusted to meet the power needs for different applications.

4.3.2. *Metro rail displacement*

The energy harvesting tie not only is able to be implemented on the freight railroad for trackside electronics, but also it can be an alternative power source for metro tracks in tunnels where suitable electrical power

Table 3
Power generation (for a single rail) under recorded tie movement of a metro rail track (30 km/h) with various loads.

Speed	Resistor		
	8 Ω	4 Ω	2 Ω
20 km/h (13 mph)	0.6 W	1.2 W	2.1 W
30 km/h (19 mph)	1.8 W	3.3 W	6.1 W

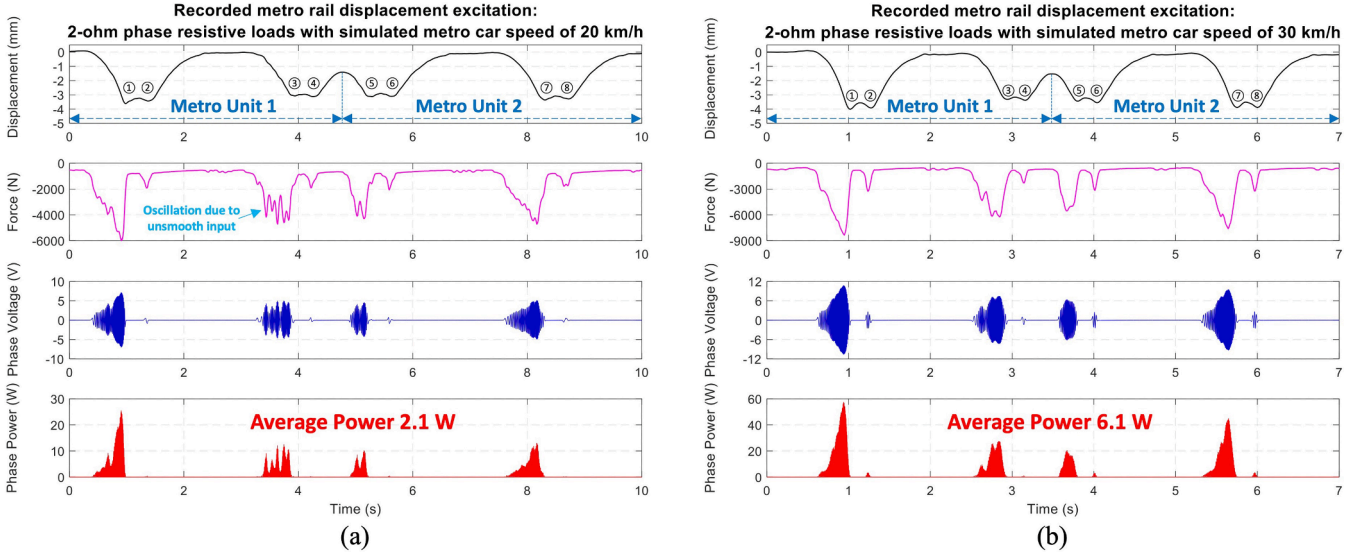

Fig. 12. Test results for the energy harvesting tie prototype with field-recorded metro rail displacements with 2 Ω resistive loads: (a) average power of 2.1 W is achieved at 20 km/h (13 mph) train speed; (b) average power of 6.1 W is achieved at 30 km/h (19 mph).

is usually inaccessible. The earlier tests are repeated with field-recorded track displacement due to a metro train in order to measure the harvested power under light wheel loads, where less track deflection is expected. The measurements are from a two-car metro train traveling at 20 km/h (13 mph) and 30 km/h (19 mph) [25]. Each car has two two-axle bogies, for a total of eight wheelsets for the train, and the metro has the operator cabs and leading bogies on each railcar at the front and rear of the train.

Experimental results under the recorded metro rail displacement with 2 Ω resistive loads are shown in Fig. 12. The displacement valleys ① - ⑧ represent maximum rail deflection under each passing wheel. The average power achieved is 2.1 W and 6.1 W for 20 km/h (13 mph) and 30 km/h (19 mph), respectively. As noted earlier and also shown in the figure, the harvester harvests power in compression and allows the track to rebound unimpeded. In this way, once the energy harvesting tie is installed on track, it is always supported by the ballast or subgrade underneath, eliminating the challenges of preload design and field installation. It is worth noting that for both simulated metro speeds, the first and last displacement valleys (i.e., ① - ② and ⑦ - ⑧) are slightly higher than the others, and so are the corresponding force and generated power. This is because of the heavier wheel loads on the leading bogies on each car, with traction motors on the wheelsets. Besides, the force oscillations between 3.5 and 4 s in Fig. 12a are caused by the unsmooth track displacement measurement, resulting in a voltage/power oscillation but also proving that the system is sensitive enough to its input. It is estimated that the oscillations are caused by the wheel-rail interface, although the precise dynamics is not pursued in this study.

Table 3 summarizes the average power harvested with field-recorded metro track displacements for various resistive loads. The average electrical power increases with decreasing resistive loading because a smaller resistive loading introduces larger electrical damping, resulting in more mechanical power being converted. The average power also increases at higher speeds due to larger rail deflection and excitation frequency. It is noticed that the metro rail displacement amplitude and frequency are less than those of freight railroad because of smaller train loads and lower speeds, so therefore, the harvested average power for metro rail with the same resistive load is less. Although less electricity generated for metro rail compared with freight rail, a doubled average power output would be estimated for a full-size prototype installed on a metro track, which is good enough to power and charge a fair number of electronic devices for condition monitoring, wireless communication, and beyond. Furthermore, since the metro track input velocity is not high, more power output, if needed, is expected if the resistive load continues to be reduced below 2 Ω.

5. Conclusions

A novel energy harvesting tie with a ball screw based half-wave rectification mechanism was designed, modeled, fabricated, and tested in the lab with sinusoidal and field-recorded track displacement measurements. Having similar dimensions to a conventional railroad tie, the energy harvesting tie can be installed readily on a track and generate electricity with every passing wheel for powering trackside sensor suites and electrical devices. The integration into a composite tie protects the embedded energy harvesters from the harsh environment, maintenance of way equipment, and vandalism and theft, significantly improving its reliability and functionality. Different from the existing bidirectional energy harvesters, the energy harvesting tie with the mechanical motion half-wave rectification mechanism harvests the track kinetic energy during its downward motion only and allows quick rebounding in the opposite direction, which releases the preload design constraints and leaves more room for design and performance improvement. A simulation study was performed based on a nonlinear model of the electrical, electromagnetic, and mechanical components to better understand the system's dynamics and predict the performance. Experiments were carried out on a fabricated half-tie prototype with both sinusoidal and field-recorded track displacements to validate the model and assess the performance of power generation. The testing results well agree with the modeling predictions, and up to 78.1% mechanical efficiency was achieved with sinusoidal excitations. Field-recorded track displacement tests demonstrated that the fabricated half-tie prototype is able to generate 16.1–44.5 W of average power from a single freight rail at 64 km/h (40 mph), and a full-size prototype is expected to double the power generation. The experiments validated that the system passed a limited amount of life cycle testing in the lab and can respond well to the low-frequency movement of the rail due to passing wheel loads. The study proves the energy harvesting tie is capable of powering various trackside electronics effectively and efficiently and has great potential to improve rail safety and connectivity by bringing more intelligence to the railroad. Future field testing is planned to explore the true lifespan of the system in the railroad environment.

CRediT authorship contribution statement

Yu Pan: Conceptualization, Methodology, Investigation, Data curation, Writing – original draft. **Lei Zuo:** Conceptualization, Supervision, Writing – review & editing, Funding acquisition. **Mehdi Ahmadian:** Conceptualization, Supervision, Writing – review & editing, Funding acquisition.

Declaration of Competing Interest

The authors declare that they have no known competing financial interests or personal relationships that could have appeared to influence the work reported in this paper.

Acknowledgment

The authors acknowledge IntegriCo Composites and Norfolk Southern for their help by providing railroad composite ties for fabrication and testing. We also greatly appreciate the funding support from the U.S. Department of Transportation University Transportation Centers (DOT-UTC) and the U.S National Science Foundation Phase II IUCRC Virginia Tech: Center for Energy Harvesting Materials and Systems (Award No. 1738689).

References

[1] Transportation Statistics Annual Report 2020. U.S. Department of Transportation, Bureau of Transportation Statistics; 2020.
[2] Train Accidents by Type and Major Cause. U.S. Department of Transportation, Federal Railroad Administration, Office of Safety Analysis; 2021.
[3] Gao M, Su C, Cong J, Yang F, Wang Y, Wang P. Harvesting thermoelectric energy from railway track. Energy. 2019;180:315–29.
[4] Hao D, Zhang T, Guo L, Feng Y, Zhang Z, Yuan Y. A high-efficiency, portable solar energy-harvesting system based on a foldable-wings mechanism for self-powered applications in railways. Energy Technol 2021;9(4):2000794. https://doi.org/10.1002/ente.v9.410.1002/ente.202000794.
[5] Pan H, Li H, Zhang T, Laghari AA, Zhang Z, Yuan Y, et al. A portable renewable wind energy harvesting system integrated S-rotor and H-rotor for self-powered applications in high-speed railway tunnels. Energy Convers Manage 2019;196:56–68.
[6] Kuang Y, Chew ZJ, Ruan T, Lane T, Allen B, Nayar B, et al. Magnetic field energy harvesting from the traction return current in rail tracks. Appl Energy 2021;292:116911. https://doi.org/10.1016/j.apenergy.2021.116911.
[7] Farritor S, Arnold R, Lu S, Hogan C. Real-time vertical track modulus measurement system from a moving railcar. Research Results, Federal Railroad Administration, RR06-08; 2006.
[8] Bowness D, Lock AC, Powrie W, Priest JA, Richards DJ. Monitoring the dynamic displacements of railway track. Proc Inst Mech Eng, Part F: J Rail Rapid Transit 2007;221(1):13–22.
[9] Vorster J, Grabe H. Axle load and track deflection on a heavy haul line. Civil Eng: Mag South African Inst Civil Eng. 2010;18:44–9.
[10] De Vos P. Railway induced vibration: state of the art report. Paris: UIC International Union of Railways; 2017.
[11] Wischke M, Masur M, Kröner M, Woias P. Vibration harvesting in traffic tunnels to power wireless sensor nodes. Smart Mater Struct 2011;20(8):085014. https://doi.org/10.1088/0964-1726/20/8/085014.

[12] Pourghodrat A, Nelson CA, Hansen SE, Kamarajugadda V, Platt SR. Power harvesting systems design for railroad safety. Proc Inst Mech Eng, Part F: J Rail Rapid Transit 2014;228(5):504–21.
[13] Cahill P, Nuallain NAN, Jackson N, Mathewson A, Karoumi R, Pakrashi V. Energy harvesting from train-induced response in bridges. J Bridge Eng 2014;19(9): 04014034. https://doi.org/10.1061/(ASCE)BE.1943-5592.0000608.
[14] Gao MY, Wang P, Cao Y, Chen R, Liu C. A rail-borne piezoelectric transducer for energy harvesting of railway vibration. J vibroeng. 2016;18(7):4647–63.
[15] Gao M, Wang P, Cao Y, Chen R, Cai D. Design and verification of a rail-borne energy harvester for powering wireless sensor networks in the railway industry. IEEE Trans Intell Transp Syst 2017;18:1596–609.
[16] Sun Y, Wang P, Lu J, Xu J, Wang P, Xie S, et al. Rail corrugation inspection by a self-contained triple-repellent electromagnetic energy harvesting system. Appl Energy 2021;286:116512. https://doi.org/10.1016/j.apenergy.2021.116512.
[17] Hou W, Li Y, Guo W, Li J, Chen Y, Duan X. Railway vehicle induced vibration energy harvesting and saving of rail transit segmental prefabricated and assembling bridges. J Cleaner Prod 2018;182:946–59.
[18] Penamalli GR. Structural health monitoring and energy harvesting for railroad [Master's Thesis]. State University of New York at Stony Brook; 2011.
[19] Wang JJ, Penamalli G, Zuo L. Electromagnetic energy harvesting from train induced railway track vibrations. In: Proceedings of IEEE/ASME International Conference on Mechatronic and Embedded Systems and Applications; 2012. p. 29–34.
[20] Pourghodrat A. Energy harvesting systems design for railroad safety [Master's Thesis]. University of Nebraska Lincoln; 2011.
[21] Zhang X, Zhang Z, Pan H, Salman W, Yuan Y, Liu Y. A portable high-efficiency electromagnetic energy harvesting system using supercapacitors for renewable energy applications in railroads. Energy Convers Manage 2016;118:287–94.
[22] Wang J, Lin T, Zuo L. High efficiency electromagnetic energy harvester for railroad application. In: ASME 2013 International Design Engineering Technical Conferences and Computers and Information in Engineering Conference; 2013. p. V004T08A37–VT08A37.
[23] Lin T, Wang JJ, Zuo L. Efficient electromagnetic energy harvester for railroad transportation. Mechatronics 2018;53:277–86.
[24] Lin T, Pan Yu, Chen S, Zuo L. Modeling and field testing of an electromagnetic energy harvester for rail tracks with anchorless mounting. Appl Energy 2018;213: 219–26.
[25] Pan Yu, Lin T, Qian F, Liu C, Yu J, Zuo J, et al. Modeling and field-test of a compact electromagnetic energy harvester for railroad transportation. Appl Energy 2019; 247:309–21.
[26] Track Safety Standards Compliance Manual. U.S. Department of Transportation, Federal Railroad Administration; 2019.
[27] Harper CA. Handbook of plastics, elastomers, and composites. McGraw-Hill Education; 2002.
[28] Thompson D. Railway noise and vibration: mechanisms, modelling and means of control. Elsevier; 2008.
[29] Guo S, Liu Y, Xu L, Guo X, Zuo L. Performance evaluation and parameter sensitivity of energy-harvesting shock absorbers on different vehicles. Veh Syst Dyn 2016;54 (7):918–42.
[30] Liu Y, Xu L, Zuo L. Design, modeling, lab, and field tests of a mechanical-motion-rectifier-based energy harvester using a ball-screw mechanism. IEEE/ASME Trans Mechatron 2017;22(5):1933–43.